The Predictive Power of Computational Astrophysics as a Discovery Tool
Proceedings IAU Symposium No. 362, 2023
D. Bisikalo, D. Wiebe & C. Boily, eds.
doi:10.1017/S1743921322001776

The predictive power of numerical simulations to study accretion and outflow in T Tauri Stars

Ana I. Gómez de Castro[1,2]

[1]Joint Center for Ultraviolet Astronomy, Universidad Complutense de Madrid, Avda. Puerta de Hierro s/n, 28040 Madrid, Spain
email: aig@ucm.es

[2]S.D. Física de la Tierra y Astrofísica, Fac. CC Matemáticas, Plaza de Ciencias 3, 28040 Madrid, Spain

Abstract. T Tauri Stars (TTSs) offer a unique chance to study the physics of non-relativistic accretion engines. In this invited talk, the current status of the field is presented with special emphasis on the predictive power of the numerical simulation of magnetospheric accretion and close binary systems and its impact on astronomical observations.

Keywords. T Tauri Stars, protostellar jets, accretion physics

1. Introduction

Gravitational engines are widely spread in astronomical environments; they are constituted by a source a gravity (a star, a compact object or a supermassive black hole) and a surrounding mass repository in the form of an accretion disk that taps the mass flow onto the gravity source. Collimated bipolar flows are generated as a self-regulating mechanism to carry away from the system part of the angular momentum excess that needs to be removed for accretion to operate. Outflows reach terminal speeds roughly equal to the Keplerian velocity at the innermost border of the disk thus, in engines driven by black holes or supermassive blackholes the outflow velocity is very close to the speed of light making these systems the most powerful engines in nature. At the other end of the energy domain are the pre-main sequence (PMS) stars with jet speeds of several hundred kilometers per second (see Table 1). These non-relativistic sources allow studying the inner structure of the engine in detail, as well as the impact of stellar and disk magnetic fields in the process.

In low mass pre-main sequence (PMS) stars (also known as T Tauri stars or TTSs) a magnetized shear layer is generated between the inner border of the disk, rotating at Keplerian velocities, and the star. The Keplerian shear amplifies the field producing a strong toroidal component; an external dynamo sets in. This toroidal field and the associated magnetic pressure push the field lines outwards from the disk rotation axis, inflating and opening them up in a *butterfly-like pattern*, so producing a current layer between the stellar and the disk dominated regions as displayed in Figure 1. Magnetic field dissipation in the current layer produces high energy radiation and particles. The magnetic link between the star and the disk is broken and reestablished continuously by magnetic reconnection. The opening angle of the current layer, as well as its extent, depends on the stellar and disk fields, the accretion rate and the ratio between the inner disk radius and the stellar rotation frequencies. Hot, pressure driven outflows are

Table 1. Gravitational engines: PMS stars compared with supermassive black holes.

Type of source	Mass of the source ($M_\odot$)	Accretion rate ($M_\odot$ yr^{-1})	Outflow velocity (km s^{-1})	Outflow mechanical power (MW)
Protostar	1	1×10^{-8}	300	6×10^{20}
Supermassive Blackhole	10^8	1	0.98c	6×10^{32}

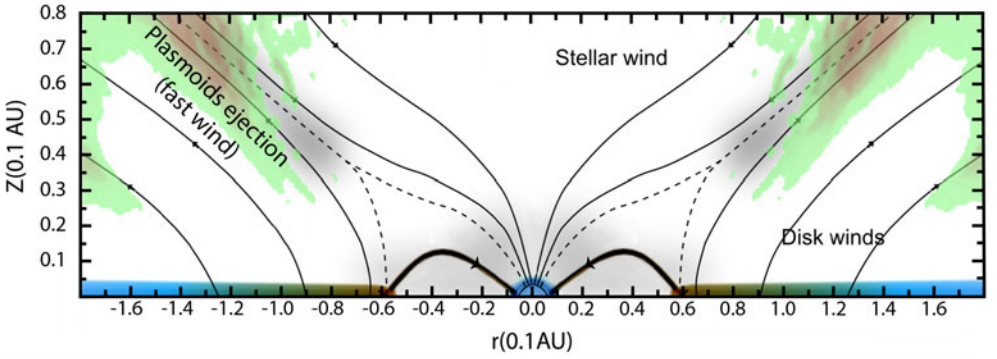

Figure 1. Sketch of the accretion engine in a PMS star. The star acts as a magnetic rotor that interacts with the plasma orbiting around it, in Keplerian orbits. The results of numerical simulations on the interaction between the stellar magnetosphere and the disk are shown; they are color coded from light green to brown and represent the emissivity of the C III] line at 191nm (Gómez de Castro & von Rekowski, 2011). The magnetic configuration is outlined as well as the reconnection layer where magnetic bubbles are thought to be generated (after Gómez de Castro et al. 2016).

produced from the star, in the region closer to the rotation axis whilst cool centrifugally driven flows are produced by the disk; plasmoids are ejected from the current layer generating a third outflowing component.

This article deals with the predictive power of the numerical simulations in this field; from the first works on protostellar jet formation (Goodson et al. 1997; Goodson & Winglee 1999) to the late developments on magnetospheric accretion (Romanova et al. 2021). In most cases, numerical simulations have just attempted to provide a physical explanation to observed phenomena but there are some few cases in which numerical simulations have been instrumental for the planning and analysis of the observations, as will be shown in the last section.

2. Numerical simulations of protostellar jets and accretion: predictions

Early in the 90's, the basic physics of the generation of bipolar collimated outflows from young stars was laid down and the two main branches of models were outlined: disk winds (Pudritz et al. 1991) and magneto-centrifugally winds from stars (Shu et al. 1994). Disk winds were first proposed by Blandford & Payne (1982) in the context of extragalactic jets from an extrapolation of the hydromagnetic solution for the fast component of the solar wind (Weber & Davis 1967). This theory was later adapted to the physics of pre-main sequence (PMS) stars and reproduced successfully some of the properties of the large scale jets (Pudritz et al. 2007). Otherwise, X-winds were based on the magnetic interaction between the star and the disk, and later evolved into the current magnetospheric accretion/launching theories (von Rekowski & Branderburg 2004, 2006). The current paradigma (as shown in Figure 1) includes both in a natural manner.

https://doi.org/10.1017/S1743921322001776 Published online by Cambridge University Press

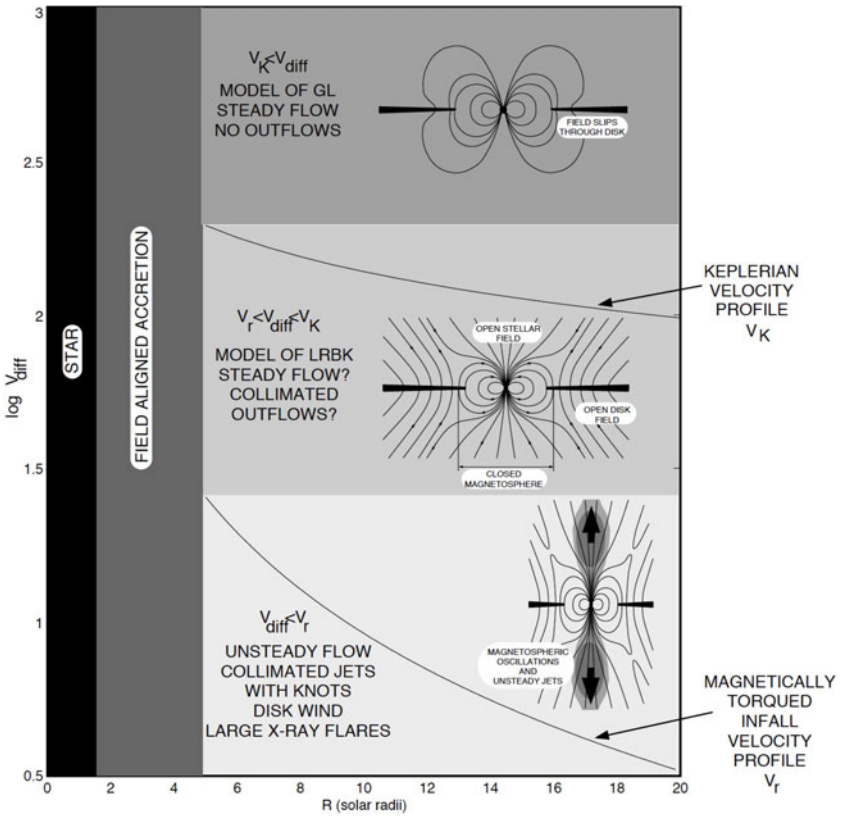

Figure 2. Summary of three classes of magnetically dominated accretion (after Goodson & Winglee 1999); v_K, v_r and v_{diff} are the keplerian, radial and diffusion velocities in the inner disk.

Early numerical models of the whole system date back to the works by Goodson et al. (1997) and Goodson & Winglee (1999). The key parameter regulating the engine is the magnetic diffusivity (ill constrained from the observations). In the high diffusivity limit, the stellar field can continuously slip through the inner disk (Ghosh & Lamb, 1979), and in the low diffusivity limit, the radial velocity is larger than the diffusion velocity and an unsteady, strong flow is initiated (Goodson et al. 1997). For intermediate diffusivities, the field wraps up until the associated magnetic pressure opens it; steady solutions are possible provided the diffusion velocity keeps being higher than the radial velocity at the inner edge of the disk (see sketch in Figure 2). In the numerical implementation of these models, often cylindrical symmetry (2.5 D) is imposed to solve the equations of the magnetohydrodynamics (MHD) and transport is hypothesized to follow the α prescription, sometimes implementing a soft dependence of α on the radius. In Goodson et al. (1997), the stellar magnetosphere is assumed to be a magnetic dipole aligned with the disk axis and the inner border of the disk is set at 8.5 R_* stellar radii. *The most important prediction from these simulations is the oscillation of the inner disk border* (being the time scale depending on the diffusivity). The time-scale and the amplitude of the oscillation of the inner border of the disk also depends on the disk density, *i.e.* on the accretion rate and the evolutionary state of the disk (Matt et al. 2002). *The prediction is that they should become more pronounced in low gas-density disks such as the transitional disks.*

Let us focus now, on the core of the engine: the interaction between the stellar magnetosphere and the disk. A major step forward was the implementation of the "cubed

https://doi.org/10.1017/S1743921322001776 Published online by Cambridge University Press

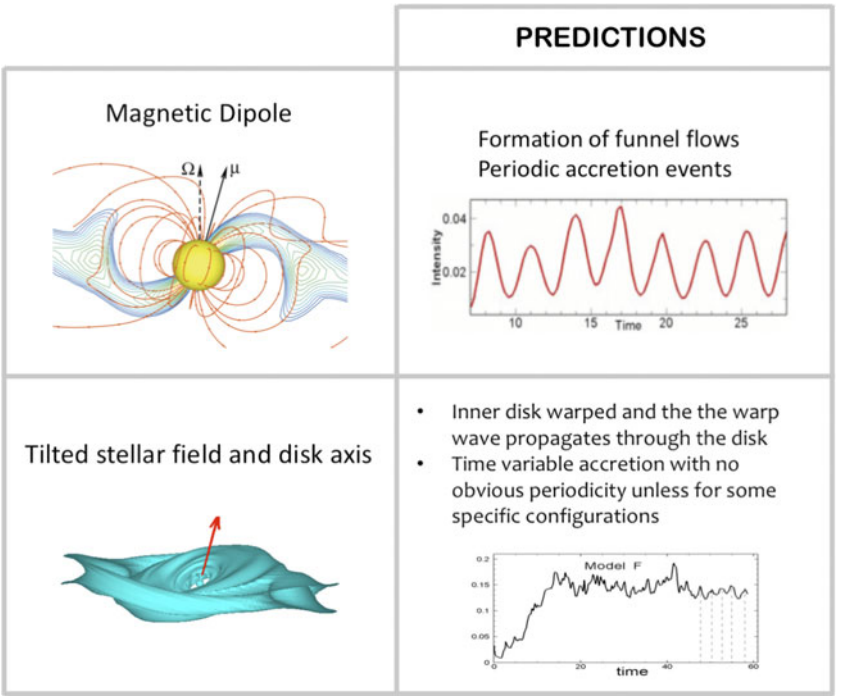

Figure 3. Some predictions of the numerical simulations of magnetospheric accretion. Top, formation of funnel flows and periodic accretion events (Romanova et al. 2004). Bottom, generation of a warp wave in the accretion disk and disapearence of the periodic accretion pattern for most of the configurations (Romanova et al. 2021).

sphere" mathematical set-up into the simulations which enabled for the first time to track the accretion flow from the inner disk onto the star (Romanova et al. 2002). The simulation was based on a clever selection of the quasi equilibrium initial conditions and solved for the accretion flow in a 2.5D, MHD framework (Romanova et al. 2003, 2004). These simple models have evolved over the years to include multipolar components in the stellar magnetic field (Long et al. 2008; Romanova et al. 2012) or allow for a misalignment between the disk axis and the magnetic rotator (Romanova et al. 2021). *A major prediction from the models is the formation of funnel flows* that channel the disk material over the stellar surface; these funnels are destroyed if the multipolar components become important. Also, accretion onto dipolar magnets produces a periodic signal due to the rotation of the star but this periodicity gets lost when multipolar components become important. As, the higher moments of the stellar magnetic field (cuadrupoles, octupoles...) decrease more pronouncedly with distance than the lower ones, it should be expected that at the distance of the inner border of the disk, the dipolar moment is the dominant. *Another interesting prediction is that tilted rotators result in the formation of a warp wave that propagates through the disk. Also accretion periodicity gets lost in most of the possible configurations* (see Figure 3).

3. Comparison between numerical predictions and observations

3.1. *Magnetospheric accretion*

Magnetospheric accretion is the most accepted theory for describing the observed characteristics of the TTSs (e.g, Hartmann et al., 2016, Gómez de Castro et al., 2013,

https://doi.org/10.1017/S1743921322001776 Published online by Cambridge University Press

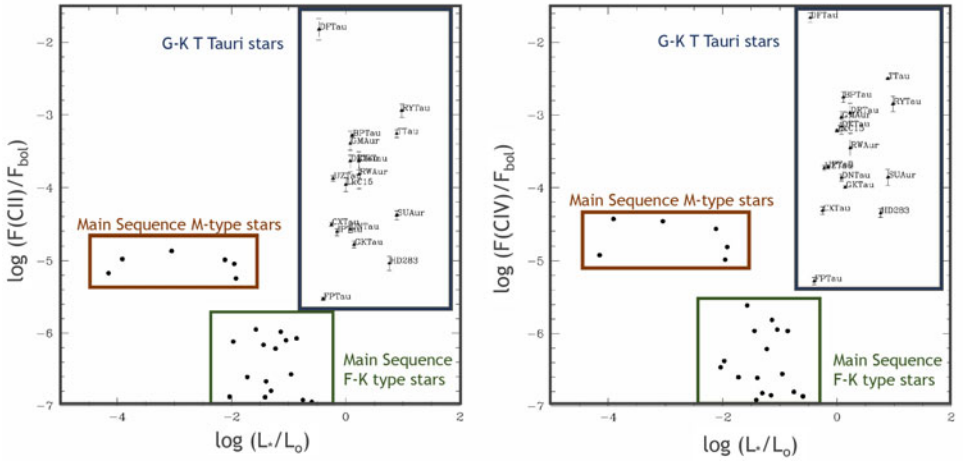

Figure 4. The normalised surface fluxes versus stellar luminosities for spectral tracers of chromospheric-like plasma ($T_e \sim 10^4$K) and plasma at $T_e \sim 4 \times 10^4$K. The location of the TTSs and the main sequence cool stars in the diagram is indicated.

Bouvier et al., 2007). Most numerical simulations hypothesize dipolar stellar magnetospheres extending up to 3-10 R_* with field strengths of ~ 1 kG. *The numerical work came after* the realization that the TTSs have extended magnetospheres and that mass infall was being channelled onto specific locations attached at the stellar surface. Actual field measurements came even later (Johns-Krull et al. 1999; Johns-Krull 2007), as well as the observation of multipolar fields (Donati et al. 2007, 2008, 2019, Gregori et al. 2012). Key observations in shaping the magnetospheric paradigma were:

• *The ultraviolet excess*: the first ultraviolet observations of the TTSs back in 80's already showed that the line fluxes produced by chromospheric and transition region tracers are 50-100 times stronger than those of their main sequence analogues (see Figure 4). This excess was used in the first estimates of an equivalent emitting volume ($2R_* - 4R_*$) and the associated magnetospheric radius driving at the first concepts of *"extended magnetospheres"*.

• *The rotational modulation of the UV flux*. Firm evidence of the rotational modulation of the UV flux came in the early 90's when several well-known TTSs were monitored to find that the light curves of some of them were rotationally modulated at UV wavelengths indicating the presence of hot spots (8,000 K - 40,000 K) on the stellar surface (Simon et al. 1990; Gómez de Castro & Fernández, 1996; Gómez de Castro & Franqueira, 1997). The detection of hot plasma localized on specific areas of the stellar surface was the first clear evidence of the existence of accretion shocks: shocks on the stellar surface where the infalling material releases its kinetic energy into heating. The stability of these locations over several rotation periods provided the first hints on the magnetospheres channelling the accretion flow. However, the actual extension of the accretion funnel has been measured only very recently, through the time lag between optical and ultraviolet observations (Espaillat et al. 2021).

• *The peculiar ultraviolet spectrum*: the atmospheres of cool stars are stratified in three main regions: the warm (T$\sim 10^4$ K) chromosphere, the hot (T$\geq 10^6$ K) corona and the transition region (TR) between them. There are well characterized correlations between the flux radiated in the various spectral tracers of these regions. These so-called flux-flux relations are used to model energy transport in cool stars and call for a universal mechanism operating in them. Flux-flux relations were also been measured in the TTSs (Yang et al. 2012; Gómez de Castro & Marcos-Arenal 2012). When compared with their

https://doi.org/10.1017/S1743921322001776 Published online by Cambridge University Press

main sequence analogues, it becomes evident that there is excess radiation from low ionization species (T$\sim 10^4$ K) with respect to the highly ionized ones (T$\sim 10^5$ K). This indicates that radiation is released by a different mechanism. The most successful models propose that the excess gravitational energy of the accreting matter is released into heating at accretion shocks where the temperature reaches 0.3-1 MK, i.e., coronal-like temperatures, driving a photoionization cascade that results in the observed scalings (Calvet & Gullbring 1998; Gómez de Castro & Lamzin 1999).

Currently, the field has reached maturity and simulations and observations have entered into the standard feedback loop to narrow down the parameter space and study other details of the system such as the dusty environment in the inner disk (see i.e. Li et al. 2022), the development of the stellar wind and the role that the combined action of the stellar wind and the magnetosphere torques may have in the acceleration of stellar rotation from the classical TTS or CTTS stage to the mildly or non-accreting sources in the weak TTS or WTTS stage (see i.e. Ireland et al. 2020 or Pantolmos et al. 2020). In most cases, numerical simulations are used rather as an analysis tool than a predictive tool.

3.2. *Enhanced velocity dispersion at high accretion rates*

A different example on the predictive value of numerical simulations comes from the expectations of the velocity dispersion at the base of the outflow; this effect is illustrated in Figure 5 for some representative engines (von Rekowski & Branderburg 2006; Gómez de Castro & von Rekowski, 2011). The simulations shown assumed cylindrical symmetry and solved the full set of resistive MHD equations to study the mass infall/outflow from an accretion disk around a star with a dipolar magnetic field aligned with the disk. Line profiles were computed for some selected spectral tracers and the basic parameters: dispersion and centroid were evaluated and represented. These calculations were made for a broad grid of models ranging from stellar fields of 1kG to 5kG, and from various assumptions on the disk magnetization (passive disk or disk with a dynamo built in). As shown in the Figure 5, the dispersion (the line broadening) grows with the field strength and with the magnetic activity of the disk. Moreover, as the spectral lines are formed in the outflow inclination effects are noticeable. However, this prediction is not fulfilled by the data; though the observed line broadenings are as high as expected for outflows from 1 kG - 2kG stars, no inclination effects are apparent implying that most of the line flux is not produced in the wind. Later on, it astronomical observations showed that such large broadenings can be produced by the magnetosphere itself.

Winds, accreting matter and the stellar atmosphere share spectral tracers in the TTSs making it difficult to disentangle the various components. However, some specific spectral lines (He II line at 164 nm or the N V resonance multiplet) are known to be radiated by the star (either by the atmosphere or by the accretion shocks). The high sensitivity of the Cosmic Origins Spectrograph (COS) in Hubble enabled to resolve the profiles of these tracers in a fair sample of TTSs and it was found that the profiles are very broad and that the broadening decreases as the stars approach the main sequence (see Figure 6).

3.3. *PMS close binaries*

Numerical simulations of the evolution of disks around PMS binaries point out that an inner gap develops within the circumbinary (CB) disk; the gap radius is about 2-3 times the semi-major axis of the orbit. The characteristics of the gap depend on the binary mass ratio, for instance, for secondary to primary mass ratios $q << 1$, the gap becomes an annular ring around the primary through which the secondary travels. It also depends on the relative mass of the secondary to the protostellar disk; if the disk mass is large compared to the mass of the secondary, inward orbital migration of the secondary may

https://doi.org/10.1017/S1743921322001776 Published online by Cambridge University Press

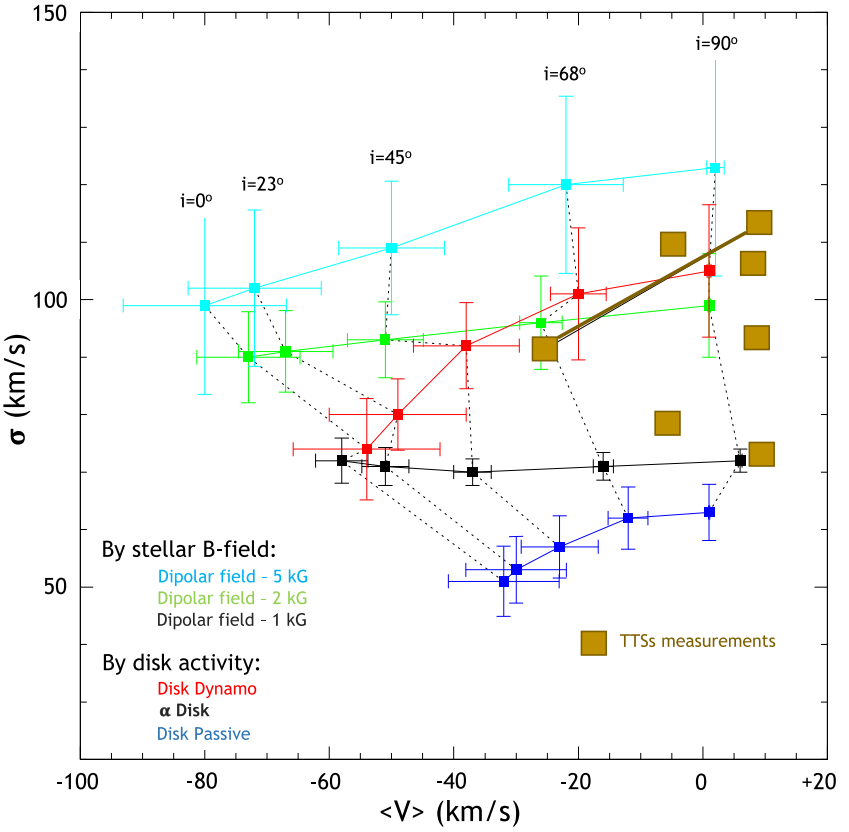

Figure 5. Velocity dispersion versus velocity centroid at the base of the jet (see Gómez de Castro & von Rekowski, 2011 for further details). The time-averaged values $\tilde{\sigma}$ and $< \tilde{V} >$ are represented as squares, while the error bars indicate the time variability during quiescence. Dark blue, black, green and light blue are used to represent the models: passive disk, matter falling onto a stellar dipolar field of 1 kG (Reference), 2kG (Mag-2kG) and 5 kG (Mag-5kG), respectively. Red is used for a magnetized disk with a dynamo built in. The *observed values* for all the TTSs observed with the HST/STIS (DE Tau, AK Sco, RY Tau, RW Aur, T Tau and RU Lup) are plotted as big brown squares. The two observations of RY Tau are plotted.).

occur on time scales comparable to the disk accretion time scale, eventually leading to collision (Lin & Papaloizou, 1993). There have been extensive theoretical studies of this situation, using both analytic and numerical methods (e.g., Goldreich & Tremaine, 1980; Lin & Papaloizou, 1986; Nelson & Papaloizou, 2003).

The inner hole excavated by the binary orbit is filled with transient dusty structures that transport the material from the inner border of the disk onto the stars. Angular momentum transport along the streamers dominates the dynamical evolution; according to hydrodynamical (HD) numerical simulations, streamers may carry as much as a 30% of the total accretion flow (Shi et al., 2012). In close PMS systems, accretion disks can either take up or release angular momentum and the details of evolution depend on the mass ratio between the two stars and on the orbit eccentricity (Artymowicz & Lubow, 1994; Bate & Bonnell, 1997, Hanawa et al., 2010, de Val Borro et al., 2011; Shi et al., 2012). Highly eccentric orbits favour the formation of spiral waves within the inner disk that do channel the flow as the accreting gas streams onto each star.

https://doi.org/10.1017/S1743921322001776 Published online by Cambridge University Press

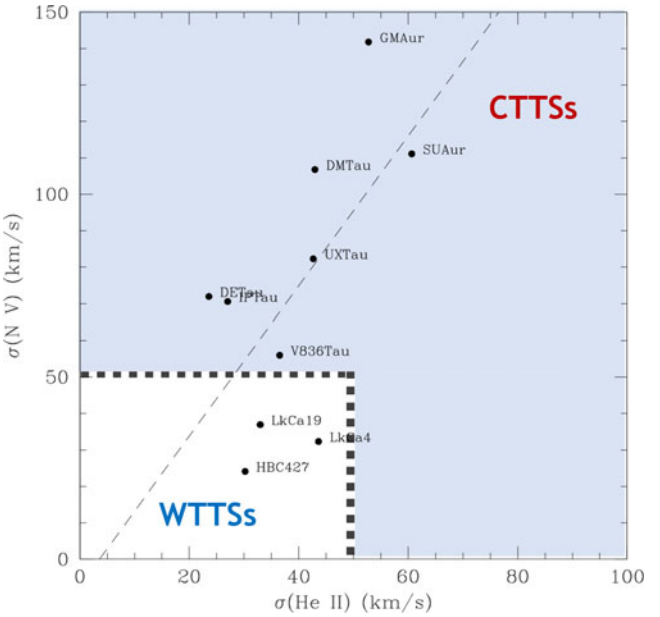

Figure 6. Broadening of the N V line (dispersion) compared with the broadening of the He II line.

For some specific orbital parameters circumstellar (CS) disks are formed around each component within the Roche Lobe; this configuration is shown in Figure 7 for the AK Sco system ($q \simeq 1$). HD simulations show that the gas flow consists of a circumbinary disk, a gap, circumstellar accretion disks, and a system of shock waves and tangential discontinuities; these elements are outlined in Figure 7. Note that the velocity distribution is non-Keplerian in the inner region of the circumbinary disk and that gas motion is governed by the bow shocks, one per star, and the gravity of the stellar components. The size and the shape of the gap are substantially determined by the bow shocks.

The study of AK Sco is a good example of the predictive power of numerical simulations. The orbit is elliptical ($e \simeq 0.47$) and the outer boundaries of the circumstellar disks (and the accretion streams passing by) get close enough at periastron passage to effectively lose the angular momentum leading to an increase of the accretion rate. Numerical results predict variations in the accretion rate *but they are not expected to be evenly distributed between the two components*; see the pronounced asymmetry in some cycles (*i.e.* cycle 12 in Figure 8). Moreover, inter-cycle variations occur in the total accretion rate, in its distribution between the components of the system, and also, in the details of the temporal evolution of the infall (see also Sytov & Fateeva, 2019 for a study of accretion under a different configuration in terms of stellar masses and eccentricity). These predictions were confirmed during the monitoring carried out with the Hubble Space Telescope. AK Sco was tracked during periastron passage in three consecutive orbits (Gómez de Castro et al. 2016; Gómez de Castro et al., 2020). Hubble UV observations show that during the first and the last cycles, the accretion rate increases at the periastron passage and the electron density becomes higher. However, not significant variations were observed during the intermediate cycle passage though the bulk UV radiation from the system increased by 20%; the different state of the system between the first two cycles at periastron passage is shown in Figure 9.

https://doi.org/10.1017/S1743921322001776 Published online by Cambridge University Press

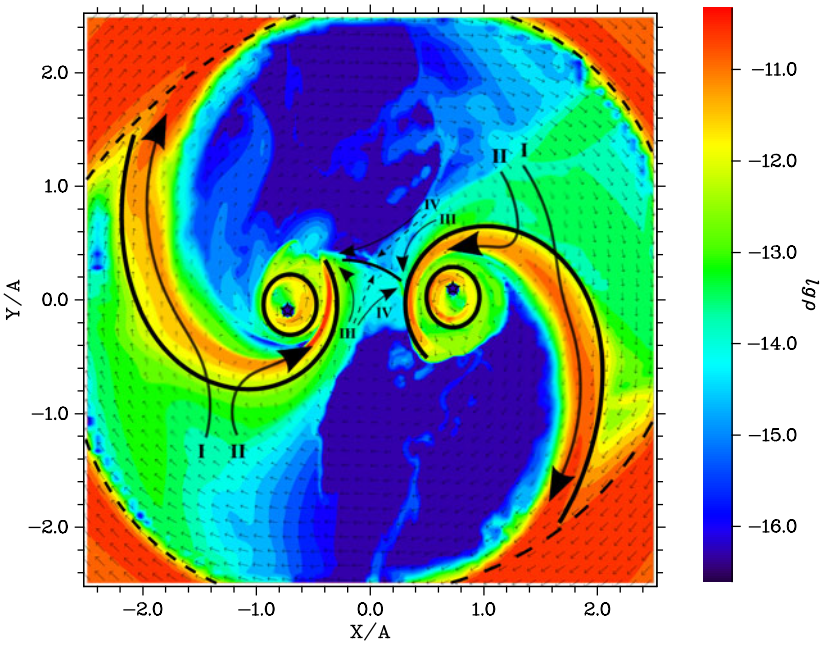

Figure 7. Generic configuration of matter distribution in a PMS close binary with q $\simeq$ 1. The stellar orbit creates a large gap within the CB disk and matter is channelled onto the stars by the variable gravitational field generated by the binary orbit. Most of the matter is transferred through streamers that connect the inner border of the CB disk to the stars. CS disks are accommodated within the Roche lobe. If the mass of the components is significantly different, only the CS disk of the primary remains estable. The main dynamical features within the gap are outlined: (I) - the outflow to the circumbinary envelope; (II) - the accretion stream; (III, IV) - parts of accretion streams that form the inner stationary shock wave and contribute to the accretion rates. The dashed line indicates the boundary of the gap. Note that the arrows mark the direction of the flow in the bow shock (from Gómez de Castro et al., 2013).

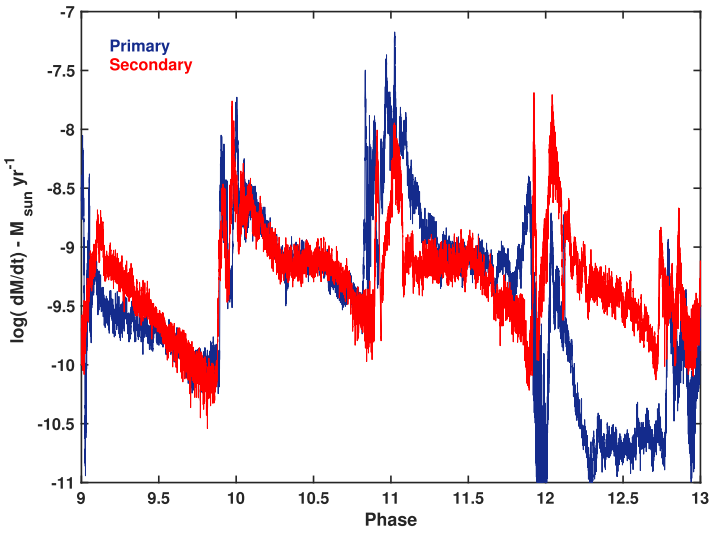

Figure 8. Predicted accretion rate onto both components of the system by HD numerical simulations of the evolution of the system (Gómez de Castro et al. 2016).

https://doi.org/10.1017/S1743921322001776 Published online by Cambridge University Press

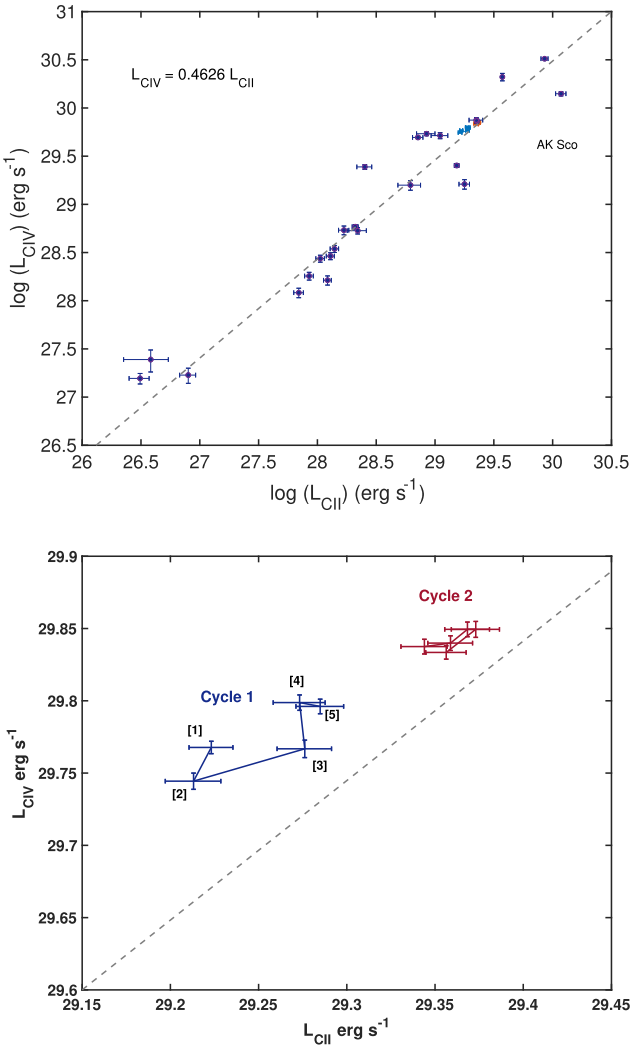

Figure 9. C IV - C II flux-flux diagram. Top, diagram for all the T Tauri stars observed with Hubble with the same configuration (STIS/G140L). AK Sco observations are plotted in blue (cycle 1) and red (cycle 2). The regression line is indicated. Bottom, zoom on the location of AK Sco observations. The order of the observations in cycle 1 is marked as [1], [2].... 1-σ error bars are plotted; note the different behaviour of the star in the two cycles (Gómez de Castro et al., 2020).

4. Summary: the predictive power of numerical simulations

Numerical simulations are a very powerful analysis tool and they are crucial for the interpretation of the data however, the physical framework needs to be clear beforehand and this comes from previous understanding, unavoidably linked to data acquisition, of the system. For instance, numerical simulation of magnetospheric accretion came roughly 10 years after the detection of hot spots on the surface of the TTSs and the evidence of the accretion shocks. However, numerical simulations are needed to predict the distribution of matter in the magnetosphere, the formation of funnel flows and to study the instabilities in the shock fronts. Also, they have contributed to disentangle the complex environment around the TTSs where the signatures of the magnetosphere, the outflow,

https://doi.org/10.1017/S1743921322001776 Published online by Cambridge University Press

and the infalling gas are observed in the same tracers. In some specific cases, such as the observation of close binary systems, numerical simulations have made detailed predictions instrumental to define the observing campaigns to test them, successfully.

References

Artymowicz, P., Lubow, S.H. 1994, *ApJ*, 421, 651

Bate, M.R., Bonnell, I.A. 1997, *MNRAS*, 288, 1041

Blandford, R. D., Payne, D.G. 1982, *MNRAS*, 199, 883

Bouvier, J., Alencar, S. H. P., Harries, T. J., Johns-Krull, C. M. et al. 2007, *Protostars and Planets V, B. Reipurth, D. Jewitt, and K. Keil (eds.), University of Arizona Press, Tucson*, 951

Calvet, N., Gullbring, E. 1998, *ApJ*, 509, 802

Donati, J. -F., Jardine, M. M., Gregory, S. G., Petit, P., et al. 2007, *MNRAS*, 380, 1297

Donati, J. -F., Jardine, M. M., Gregory, S. G., Petit, P., et al. 2008, *MNRAS*, 386, 1234

Donati, J. -F., Bouvier, J., Alencar, S. H., Hill, C., et al. 2019, *MNRAS*, 483, L1

de Val-Borro, M., Gahm, G. F., Stempels, H. C, et al. 2011, *A&A*, 535, 6

Ghosh, P., Lamb, F.K. 1979, *ApJ*, 232, 259

Goldreich, P.,S., Tremaine, S. 1980, *ApJ*, 241, 425

Gómez de Castro, A. I., Fernández, M. 1996, *MNRAS*, 283, 55

Gómez de Castro, A. I., Franqueira, M. 1997, *A&A*, 323, 541

Gómez de Castro, A. I., Lamzin, S. 1999, *MNRAS*, 304, L41

Gómez de Castro, A. I., von Rekowski, B. 2011, *MNRAS*, 411, 849

Gómez de Castro, A. I., Marcos-Arenal, P. 2012, *ApJ*, 749, 190

Gómez de Castro, A. I. 2012, *ApJ*, 775, 131

Gómez de Castro, A. I. 2013, *Planets, Stars and Stellar Systems Vol. 4, by Oswalt, Terry D.; Barstow, Martin A.*, 279

Gómez de Castro, A.I., Gaensicke, B., Neiner, C. & Barstow, M.A. 2016a, *JATIS*, 2, id. 041215

Gómez de Castro, A.I., Loyd, R. O. P., France, K., Sytov, A. et al. 2016b, *ApJ*, 818, L17

Gómez de Castro, A. I., Vallejo, J. C., Canet, A., Loyd, P. et al. 2020, *ApJ*, 904, 120

Goodson, A. P., Winglee, R. M., Bohm, K.-H. 1997, *ApJ*, 489, 199

Goodson, A. P., Winglee, R. M. 1999, *ApJ*, 524, 159

Gregory, S. G., Donati, J. -F., Morin, J., Hussain, G. A. J., et al. 2012, *ApJ*, 755, 97

Hanawa, T., Ochi, Y., Ando, K. 2010, *MNRAS*, 708, 485

Hartmann, L., Herczeg, G., Calvet, N. 2016, *ARAA*, 54, 135

Ireland, L. G., Zanni, C., Matt, S. P., Pantolmos, G. 2021, *ApJ*, 906, 4

Johns-Krull, C. M., Valenti, J. A.; Koresko, C. 1999, *ApJ*, 516, 900

Johns-Krull, C. M. 2007, *ApJ*, 664, 975

Li, R., Chen, Y.-X. L., Douglas N. C. 2022, *MNRAS*, 510, 5246

Lin, D.N.C., Papaloizou, J.C.B. 1992, *Protostars and planets III (A93-42937 17-90)*, 749

Long, M., Romanova, M. M., Lovelace, R. V. E. 2008, *MNRAS*, 386, 1274

Matt, S., Goodson, A. P., Winglee, R. M. 2002, *ApJ*, 574, 232

Nelson, R.P., Papaloizou, J.C.B. 2003, *Proceedings of the Conference on Towards Other Earths: DARWIN/TPF and the Search for Extrasolar Terrestrial Planets, Edited by M. Fridlund, T. Henning, compiled by H. Lacoste*, ESA SP-539, 175

Pantolmos, G., Zanni, C., Bouvier, J. 2020, *A&A*, 643, A129

Pudritz, R. E., Pelletier, G., Gómez de Castro, A. I. 1991, *The Physics of Star Formation and Early Stellar Evolution, NATO Advanced Study Institute (ASI) Series C*, 342, 539

Pudritz, R. E., Ouyed, R., Fendt, Ch., Brandenburg, A. 2007, *Protostars and Planets V, B. Reipurth, D. Jewitt, and K. Keil (eds.), University of Arizona Press, Tucson*, 277

Romanova, M. M., Ustyugova, G. V., Koldoba, A. V., Lovelace, R. V. E. 2002, *ApJ*, 578, 420

Romanova, M. M., Ustyugova, G. V., Koldoba, A. V., Wick, J.V., et al. 2003, *ApJ*, 595, 1009

Romanova, M. M., Ustyugova, G. V., Koldoba, A. V., Lovelace, R. V. E. 2004, *ApJ*, 610, 910

Romanova, M.M., Kulkarni, A.K., Long, M., & Lovelace, R.V.E. 2008, *AIP Conference Proceedings*, 1068, 87

Romanova, M. M., Ustyugova, G. V., Koldoba, A. V., Lovelace, R. V. E. 2012, *MNRAS*, 421, 63
Romanova, M. M., Koldoba, A. V., Ustyugova, G. V., Blinova, A. A. et al. 2021, *MNRAS*, 506, 372
Simon, T., Vrba, F. J., Herbst, W. 1990, *AJ*, 100, 1957
Shi, J.-M., Krolik, J.H., Lubow, S.H. et al. 2012, *ApJ*, 749, 118
Shu, F., Najita, J., Ostriker, E., Wilkin, F. et al. 1994, *ApJ*, 429, 781
Sytov, A. Yu., Fateeva, A.M. 2021, *ARep*, 63, 1045
von Rekowski, B., Brandenburg, A. 2006, *AN*, 327, 53
von Rekowski, B., Brandenburg, A. 2004, *A&A*, 420, 17
Weber, E.J., Davis, L. 1967, *ApJ*, 148, 217
Yang, H., Herczeg, G. J., Linsky, J.L., Brown, A. et al. 2012, *ApJ*, 744, 121

Discussion

QUESTION 1: I have a question concerning the topology of the magnetic field. What sets the footpoints of the outermost closed magnetic field lines, is it only the rotation or spin of the T Tauri star or is it also the relative amplitude of the momentum of the magnetic field of the star? How far is it with respect to the corotation radius?

ANSWER: The location depends both on the stellar magnetic field (including the details of the field topology and orientation) but also on the rotation velocity and the diffusivity of the material in the inner disk. Its location is ill determined from observations.

QUESTION 2: I am interested in the hot spot from accretion. Some people claim that the structure can be viewed by some recent observations not by light cap but by others, some method like obscuration or others. Do you have comments on that?

ANSWER: You see the spot basically at any time; it is very difficult not to see the accretion area. What it is difficult to separate the contribution from the hot spot from the rest of the atmosphere, since it shares similar spectral tracers. Monitoring and rotational modulation provide the best chances to pick out the contribution from the spot.

https://doi.org/10.1017/S1743921322001776 Published online by Cambridge University Press